Time-variable gravity fields and ocean mass change from 37 months of kinematic Swarm orbits

Christina Lück[1], Jürgen Kusche[1], Roelof Rietbroek[1], and Anno Löcher[1]

[1]Institute of Geodesy and Geoinformation, University of Bonn, Bonn, Germany

Correspondence to: lueck@geod.uni-bonn.de

Abstract. Measuring the spatiotemporal variation of ocean mass allows one to partition volumetric sea level change, sampled by radar altimeters, into a mass-driven and a steric part, the latter being related to ocean heat change and the current Earth's energy imbalance. Since 2002, the Gravity Recovery and Climate Experiment (GRACE) mission provides estimates of the Earth's time-variable gravity field, from which one can derive ocean mass variability. However, GRACE has reached the end of its lifetime with data degradation and several gaps during the last years, and there will be a prolonged gap until the launch of the follow-on mission GRACE-FO. Therefore, efforts focus on generating a long and consistent ocean mass time series by analyzing kinematic orbits from other low-flying satellites; i.e. extending the GRACE time series.

Here we utilize data from the European Space Agency's (ESA) Swarm Earth Explorer satellites to derive and investigate ocean mass variations. We investigate the potential to bridge the gap between the GRACE missions and to substitute missing monthly solutions. Our monthly Swarm solutions have a root mean square error (RMSE) of 4.0 mm with respect to GRACE, whereas directly estimating trend, annual and semiannual signal terms leads to an RMSE of only 1.7 mm. Concerning monthly gaps, our Swarm solution appears better than interpolating existing GRACE data in 13.5 % of all cases, for 80.0 % of all investigated cases of an 18-months-gap, Swarm ocean mass was found closer to the observed GRACE data compared to interpolated GRACE data. Furthermore, we show that precise modelling of non-gravitational forces acting on the Swarm satellites is the key for reaching these accuracies. Our results have implications for sea level budget studies, but they may also guide further research in gravity field analysis schemes, including non-dedicated satellites.

1 Introduction

Sea level rise, currently about 3 mm yr^{-1} in global average, will affect many countries and communities along the world's coastlines, with potentially devastating consequences (Nicholls and Cazenave, 2010; Stocker et al., 2013). Knowing ocean mass change is important because it enables the partitioning of volumetric sea level changes, as measured by radar altimeters, into mass and steric parts. The steric sea level change is related to ocean heat content and thus to the question whether the Earth's energy imbalance (currently 0.9 W m^{-2}, Trenberth et al. 2014) can be explained. Yet, a number of studies found differing ocean mass rates from the GRACE data sets (Rietbroek et al., 2016; Cazenave and Llovel, 2010; Lombard et al., 2007; Gregory et al., 2013; Llovel et al., 2014). Therefore, and considering the gap between the GRACE missions, alternative

methods to derive ocean mass changes are expected to provide valuable insights.

The European Space Agency (ESA) Swarm Earth Explorer mission was successfully launched into a near-polar low Earth
orbit (LEO) on November 22, 2013. The three identical satellites, referred to as Swarm A, Swarm B and Swarm C, were
5   designed to provide the best-ever survey of the geomagnetic field and its temporal variability. For this aim, the satellites are
equipped with absolute scalar and vector field magnetometers. Furthermore, a suprathermal ion imager and a Langmuir Probe
provide information about the Earth's electric field. The attitude of each satellite is measured by star trackers with three cam-
era head units. For Precise Orbit Determination (POD), each spacecraft is equipped with an 8-channel dual-frequency GPS
receiver (Zangerl et al., 2014) and laser retroreflectors that allow satellite laser ranging (SLR) for orbit validation. Also, all
10   three satellites carry accelerometers for deriving the drag force, which would have been helpful in gravity field determination.
However, these measurements were found to exhibit spurious signals, mostly thermal related, and cannot be used in a straight-
forward way. Siemes et al. (2016), after reprocessing, provide corrected non-gravitational accelerations in along-track direction
for Swarm C, but it is unclear whether such corrections will be ever derived for all components.

15   Swarm A and C fly side by side in a mean altitude of 450 km while the Swarm C orbit is at 515 km; this results in a
drifting of Swarm C's orbital plane with respect to the other two planes. This constellation, together with the global coverage
due to near-polar and near-circular orbits, provides the basis for gravity field recovery. This has sparked a renewed interest in
satellite gravity method development, in particular since the Gravity Recovery and Climate Experiment (GRACE) has reached
the end of its lifetime and its follow-on GRACE-FO will be launched only in spring 2018. At the time of writing, kinematic
20   LEO orbits are considered as a promising option for deriving global gravity fields during a GRACE mission gap (Rietbroek
et al., 2014). Several Swarm simulation studies had already been conducted before launch, e.g. Gerlach and Visser (2006) and
Visser (2006). Wang et al. (2012), using the energy integral approach, suggested that static gravity solutions could be derived
up to degree 70 from Swarm-like constellations, while time-variable monthly fields might be recovered up to degree 5 to 10.
These authors furthermore hypothesized that the use of kinematic baselines would increase the spatial resolution, albeit at the
25   expense of weaker solutions at longer wavelengths. Consequently, after launch, kinematic GPS orbits have been derived and
used by different groups to estimate time-variable gravity fields: Teixeira da Encarnação et al. (2016) compare solutions of the
Astronomical Institute of Bern (AIUB, Jäggi et al. 2016), the Astronomical Institute of the Czech Academy of Science (ASU,
Bezděk et al. 2016) and the Institute of Geodesy (IFG) of the Graz University of Technology, suggesting that a meaningful
time-varying gravity signal can be derived until degree 12.

30

In this study, we first compute a set of in-house time-variable gravity fields from Swarm kinematic orbits to further derive
a time series of ocean mass change. To this end, we use the integral equation approach developed earlier at the University of
Bonn (Mayer-Gürr, 2006) and compare time series of monthly Swarm solutions and annual/trend solutions to existing GRACE
solutions. We model non-gravitational accelerations (drag, solar radiation and Earth radiation pressure) for all three Swarm

	product	sampling	availability	reference frame
Kinematic Orbits	ESA Level 2 KIN (van Den IJssel)	10s	December 1st, 2013 to July (A:15th., B:15th., C:10th.), 2014	ITRF 2008
Kinematic Orbits	ESA Level 2 KIN (van Den IJssel)	1s (10s is used)	July (A:15th., B:15th., C:10th.), 2014 to December 31st, 2016	ITRF 2008
Star Camera	ESA Level 1b	1s (10s is used)	December 1st, 2013 to December 31st, 2016	ITRF 2008 to satellite frame

Table 1. Utilized orbit and star camera data.

satellites which is found to be important to improve the gravity results.

This article is organized as follows: In Sect. 2 we describe the used data sets and background models, followed by a brief discussion of methods in Sect. 3. Section 4 will present our results for ocean mass change, discuss the effects of non-gravitational
5 force modelling and gravity field parameterization, and the relative contribution of the three satellites.

2 Data

2.1 Swarm data

Time series of quality-screened, calibrated and corrected measurements are provided in the Swarm Level 1b products. The Swarm Satellite Constellation Application and Research Facility (SCARF, Olsen et al. 2013) further processes Level 1b data
10 and auxiliary data to Level 2 products. Here we use Level 2 kinematic orbits (van den IJssel et al., 2015, 2016), see Table 1, and Level 1b star camera data which are required for transforming from the terrestrial to satellite reference frame.

For modelling non-conservative forces, we implemented a Swarm macro model consisting of area, orientation and surface material for 15 panels, supplemented with surface properties such as diffuse and specular reflectivity for computing solar and
15 Earth radiation pressure (ESA, Christian Siemes, personal communication).

2.2 Background models

During gravity field recovery, we used the GOCO05c model (Pail et al., 2016) complete to degree 360 as a mean background field. All time-variable background models (cf. Table 2) are consistent with GRACE RL05 processing standards (Dahle et al.,
20 2012) except for the atmospheric tides which were chosen such as to be aligned with ITSG Graz solutions. The reason for this is that we compare our Swarm solutions to the monthly ITSG-Grace2016 solutions (Mayer-Gürr et al., 2016).

Background model	Product
Static Field	GOCO05c
Earth Rotation	IERS2010
Moon, Sun and Planets	JPL DE421
Earth Tide	IERS2010
Ocean Tide	EOT11a
Pole Tide	IERS2010
Ocean Pole Tide	Desai2004
Atmospheric Tides	van Dam / Ray
Atmosphere and Ocean Dealiasing	AOD1B RL05
Permanent Tidal Deformation	included (zero tide)

Table 2. Background models used during the processing

2.3 Density model

Drag modelling requires knowing the thermospheric density and temperature. In this work, we make use of the empirical NRLMSISE-00 model (Picone et al., 2002). NRLMSISE-00's data base includes total mass density from satellite accelerometers and POD, temperature from incoherent scatter radar as well as molecular oxygen number density, however collected under

5   different solar activity conditions. The model is driven by observed solar flux (F10.7 index) and geomagnetic index (A_P). In Vielberg et al. (subm.) we compare NRLMSISE-00 to GRACE-derived thermospheric density and derive an empirical correction for this model; this has not yet been applied here.

3 Methods

In order to address our central question - to what extent will Swarm enable one to infer ocean mass change - we first compute

10   time-variable gravity fields from kinematic orbits, while considering different processing options. Then, ocean mass is derived from the computed Stokes coefficients (e.g. Chambers and Bonin, 2012), and results will be compared to the GRACE solutions. In the following, we describe our modelling of the non-conservative forces (Sect. 3.1), the processing method (integral equation approach with short arcs), and two options for gravity field parameterization within the gravity recovery: (1) estimation of monthly fields (2) estimation of a trend, annual and semiannual model for each harmonic coefficient from the whole mission

15   lifetime in a single adjustment (Sect. 3.2). Finally, results are compared to the GRACE solution in terms of area averages for the total ocean as well as - for comparison - to water storage change within various large terrestrial river basins (Sect. 3.3).

3.1 Modelling of non-gravitational forces

While all three Swarm satellites carry accelerometers intended to support POD and the study of the thermosphere, unfortunately these data have turned out as severely affected by sudden bias changes ("steps"), temperature-induced bias variations,

acceleration spikes due to thruster activations, and failures of automatically detecting and correcting errors.

Siemes et al. (2016) developed a method to clean and calibrate the along-track acceleration of Swarm C. However, Swarm A and B, as well as the other C directions have stronger problems and it is not clear whether these data can be used in the future. In the light of recent improvements of empirical thermosphere models (Vielberg et al., subm.) and seen that we require

5   all three components of non-conservative acceleration $\mathbf{a}_{model}$ for gravity recovery, we decided to rather model them, using the well-known relation

$$\mathbf{a}_{model} = \mathbf{a}_{drag} + \mathbf{a}_{SRP} + \mathbf{a}_{ERP}. \tag{1}$$

$\mathbf{a}_{model}$ is the sum of atmospheric drag $\mathbf{a}_{drag}$, solar radiation pressure $\mathbf{a}_{SRP}$ and Earth radiation pressure $\mathbf{a}_{ERP}$. We will briefly summarize our implementation below.

Atmospheric Drag:

Atmospheric drag is commonly taken into account by evaluating

$$\mathbf{a}_{drag} = C_d \frac{A_{ref}}{2m} \rho v_r^2 \hat{\mathbf{v}}_r, \tag{2}$$

where A_{ref} is the surface area of the spacecraft, m its mass, ρ the thermospheric density (here from NRLMSISE-00), v_r the

15   velocity of the satellite relative to the atmosphere, and $\hat{\mathbf{v}}_r$ the normalized velocity vector. The drag coefficient C_d depends on density, temperature and the macro model properties and we follow Doornbos (2011) in its computation.

Solar Radiation Pressure:

Solar radiation is absorbed or reflected at the satellite's walls, leading to an acceleration (Sutton, 2008; Montenbruck and Gill,

20   2005)

$$\mathbf{a}_{SRP} = \sum_{i=1}^{N} -\nu \frac{1AU^2 R A_i \cos\left(\Phi_{inc,i}\right)}{r_\odot^2 m} \left[2\left(\frac{C_{rd,i}}{3} + c_{rs,i} \cos\left(\Phi_{inc,i}\right) \right) \hat{\mathbf{n}}_i + (1 - c_{rs,i})\hat{\mathbf{s}} \right]. \tag{3}$$

Equation 3 accumulates SRP for each of the N plates of the macro model. R is the solar flux constant valid at distance of 1 astronomical unit (AU), A_i is the area of the ith plate and $c_{rd,i}$ and $c_{rs,i}$ are the diffuse and specular reflectivity coefficients. $\Phi_{inc,i}$ denotes the angle between the the Sun (unit vector $\hat{\mathbf{s}}$) and the normal vector of each panel $\hat{\mathbf{n}}_i$. The shadow function ν

25   varies between 0 when the satellite is in eclipse and 1 if it is fully illuminated. The term $1AU^2/r_\odot^2$ accounts for the eccentricity of the Earth's orbit, with $r_\odot$ being the varying Sun-satellite distance.

Earth Radiation Pressure:

Radiation emitted from the Earth's surface (ERP) is taken into account similar to solar radiation pressure:

30   $$\mathbf{a}_{ERP} = \sum_{i=1}^{N} \sum_{j=1}^{M} -\frac{R^j A_i \cos\left(\Phi_{inc,i}^j\right)}{m} \left[2\left(\frac{C_{rd,i}}{3} + c_{rs,i} \cos\left(\Phi_{inc,i}^j\right) \right) \hat{\mathbf{n}}_i + (1 - c_{rs,i})\hat{\mathbf{s}}^j \right]. \tag{4}$$

The satellite's footprint is divided into M sections and R^j takes into account the effect of albedo and emission (we use the Cloud and the Earth's Radiant Energy System (CERES) dataset EBAF-TOA Ed2.8 that provides monthly values). Different from the conventional implementation (Knocke et al., 1988), we expanded these data into a low-degree spherical harmonic representation to account for longitudinal variations.

3.2 Gravity field estimation

For gravity field estimation, we use the integral equation approach (Schneider, 1968; Reigber, 1969). Kinematic orbits are partitioned into (short) arcs and each observed 3D position $\mathbf{r}(\tau)$ between the arc's begin and end ($\mathbf{r}_A$ and $\mathbf{r}_B$) can be expressed as

$$\mathbf{r}(\tau) = \mathbf{r}_A(1-\tau) + \mathbf{r}_B\tau - T^2 \int_0^1 K(\tau,\tau')\mathbf{f}(\tau')d\tau', \tag{5}$$

with normalized time τ and the integral kernel

$$K(\tau,\tau') = \begin{cases} \tau'(1-\tau) & \text{for } \tau' \leq \tau \\ \tau(1-\tau') & \text{for } \tau' > \tau. \end{cases} \tag{6}$$

In other words, $T^2 \int_0^1 K(\tau,\tau')\mathbf{f}(\tau')d\tau'$ in Eq. 5 represents the offset of the current position from a straight line connecting $\mathbf{r}_A$ and $\mathbf{r}_B$, caused by gravitational and non-gravitational forces $\mathbf{f}(\tau')$. After discretization (sampling rate of kinematic orbits is 1 second after July 2014), one can write the above as an adjustment problem with two groups of solved-for parameters:

$$\mathbf{y} = \begin{bmatrix} \mathbf{r}_A \\ \mathbf{r}_B \\ \mathbf{acc}_{perArc} \end{bmatrix} \text{ and } \mathbf{x} = \begin{bmatrix} c_{20} \\ c_{21} \\ s_{21} \\ \vdots \\ s_{nn} \\ \mathbf{acc}_{global} \end{bmatrix}. \tag{7}$$

$\mathbf{y}$ contains all arc-related parameters, which can be eliminated during the estimation. These include initial and final position of each arc and additional parameters such as accelerometer bias or scale factors. The gravity field parameters are then collected in $\mathbf{x}$. For more details of the integral equation approach, see Mayer-Gürr (2006) and Löcher (2010).

In this study, we consider two different ways of parameterizing the gravity field: (1) To be consistent with GRACE, we estimate monthly spherical harmonic coefficients complete to varying low degrees. (2) In a single adjustment, a set of trends and (semi)annual harmonic amplitudes are additionally estimated for each Stokes coefficient, which is likely more reasonable when aiming at a long and stable time series:

$$
\begin{aligned}
c_{nm}(t) &= \bar{c}_{nm} + \dot{c}_{nm}(t - t_0) \\
&+ c_{nm}^{c_1} \cos\left(2\pi \frac{t - t_0}{yr}\right) + c_{nm}^{s_1} \sin\left(2\pi \frac{t - t_0}{yr}\right) \\
&+ c_{nm}^{c_2} \cos\left(4\pi \frac{t - t_0}{yr}\right) + c_{nm}^{s_2} \sin\left(4\pi \frac{t - t_0}{yr}\right) \\
s_{nm}(t) &= \bar{s}_{nm} + \dot{s}_{nm}(t - t_0) \\
&+ s_{nm}^{c_1} \cos\left(2\pi \frac{t - t_0}{yr}\right) + s_{nm}^{s_1} \sin\left(2\pi \frac{t - t_0}{yr}\right) \\
&+ s_{nm}^{c_2} \cos\left(4\pi \frac{t - t_0}{yr}\right) + s_{nm}^{s_2} \sin\left(4\pi \frac{t - t_0}{yr}\right).
\end{aligned}
\tag{8}
$$

To prevent force modelling errors, e.g. from biases and sampling problems with the thermosphere density model and macro model errors, from propagating into the gravity field estimates, it is common to introduce additional parameters. Here we co-estimate an "accelerometer bias" per arc and per axis, either as a constant value or in form of a low-degree polynomial. While we found this usually sufficient, we also performed tests with an additional global scaling factor per axis. Another possibility would be to also co-estimate the bias globally; in that case a polynomial of slightly higher degree could be appropriate. The influence of this "accelerometer parameterization" will be evaluated in the course of this paper, yet one needs to bear in mind that these parameters rather measure force model inconsistencies and should not be mixed up with instrument errors. We furthermore investigate the influence of different arc lengths (which controls the temporal acceleration parameterization) as well as the effect of spherical harmonic truncation.

3.3 Ocean mass changes and river basin averages

As was mentioned already, we choose different regions for our investigation (see Fig. 1), but our focus is on the total ocean in order to test the hypothesis that Swarm can bridge the GRACE ocean mass time series.

For computing smoothed basin mass averages, let $F(\lambda, \Phi)$ be the equivalent water height (EWH), derived from the spherical harmonics (Wahr et al., 1998). The smoothed region average $\overline{F}_{O_W}$ over the region O can be expressed as

$$
\overline{F}_{O_W} = \frac{1}{\overline{O}_W} \int_\Omega O_W(\lambda, \theta) F \, dw,
\tag{9}
$$

with the smoothing Kernel W, here a 500 km Gaussian filter. The integral is effectively evaluated for the smoothed area function $O_W(\lambda, \theta)$,

$$
O_W(\lambda, \theta) = \sum_{n=0}^{\infty} \sum_{m=-n}^{n} \overline{O}_{nm}^W \overline{Y}_{nm}(\lambda, \theta) = \frac{1}{4\pi} \int_\Omega W(\lambda, \theta, \lambda', \theta') O(\lambda', \theta') \, dw'.
\tag{10}
$$

Some postprocessing needs to be applied to the estimated gravity fields, depending on the intention. As we compare our results to the monthly GRACE solutions, we may or may not replace the c_{20} coefficient with those derived from satellite laser
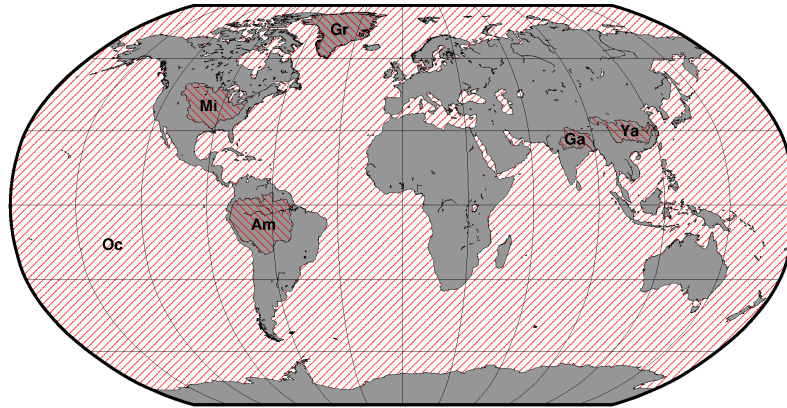
Figure 1. Areas of investigation: ocean (OC), Amazon (AM), Mississippi (MI), Greenland (GR), Yangtze (YA) and Ganges (GA).

	arc length [minutes]	non-grav. acc.	bias	scale	maximum d/o
monthly	30	modelled	constant per arc (pA0)	none	estimated until 40, evaluated until 12
trend+annual+semiannual	45	modelled	constant+trend per arc (pA1)	none	static until 40, time-variable until 12

Table 3. Parameterization for our monthly solutions and for our estimation of trend+annual+semiannual signal terms. All results are subject to a 500 km Gaussian filter.

ranging (SLR) (Cheng et al., 2013). While replacing c_{20} leads to a workflow more in line with GRACE, keeping the Swarm-derived c_{20} would answer the question whether Swarm alone is able to measure mass change. In a next step, we substitute all degree 1 coefficients to correct for geocenter motion (Swenson et al., 2008), which cannot be detected with the current GRACE and Swarm processing. We apply a correction for glacial isostatic adjustement following A et al. (2013), but as long as we apply the same correction to GRACE our results are independent of this choice. Finally, we decided on an ocean mask excluding a coastal buffer zone and to also use data over the Arctic Ocean.

4   Results

If not stated otherwise, we used the parameterization in Table 3 for monthly ocean mass or ocean mass from a direct estimation of trend, annual and semiannual signal terms is shown. Our test studies include all possible combinations of the parameterizations shown in Table 4, which leads to more than 500 configurations.

arc length [minutes]	non-grav. acc.	bias	scale	maximum d/o
30	not modelled	none	none	monthly: estimated until 20/40, evaluated until 10/12/14
45	modelled	constant per arc (pA0)	global	static part until 20/40/60, time-variable part until 10/12/14
60		constant+trend per arc (pA1)		
		constant global (global0)		
		polyn. of deg. 4 global (global4)		

Table 4. Parameterizations that have been tested in this study.

4.1 Ocean mass from GRACE and Swarm

Figure 2 shows monthly ocean mass change in mm EWH derived from GRACE as a reference and from different Swarm TVG solutions from AIUB, ASU, IGG and ITSG (processing details can be found in Table 5). The IGG time-variable gravity field was computed with an arc length of 30 minutes and with modelled non-gravitational accelerations, with a constant bias per arc and direction being co-estimated, which leads to our best solution. All Swarm time series show a behavior similar to the GRACE solution, but they appear overall noisier, as can be seen from the root mean square (RMS) values in Table 6. The quality of all solutions improves after the GNSS receiver update in July 2014. It is furthermore interesting to compute the RMSE of all solutions when we assume the GRACE solution to be the truth (first row of Table 6). The ASU time series has the lowest RMSE of 2.8 mm; it is closest to GRACE. The IGG solution has the second lowest RMSE of 4.0 mm and is still very close to GRACE. To assess the spread between the different Swarm solutions, we compute the RMSE for each combination (off-diagonal of Table 6) which is of the same magnitude as the RMSEs of GRACE and Swarm.

An important issue in extending the ocean mass time series is the accuracy of the trend. Table 7 shows the trends as well as the amplitude and phase of the Swarm solutions. The trend of the IGG solution (3.3 mm yr^{-1}) is the closest to GRACE (3.5 mm yr^{-1}). While the trend over three years itself cannot be considered as representative for the GRACE era due to interannual variability of barotropic modes, this suggests that Swarm data could be used to bridge a gap between GRACE and GRACE-FO.

Figure 3 shows the degree variances and the difference degree variances of GRACE and our IGG solution for May 2016. Obviously, the higher the degree, the higher is the discrepancy between GRACE and Swarm. The difference (dotted gray line) indicates that Swarm is only reliable for degrees up to about 12. The formal errors (dotted black line) appear to be too optimistic, as they are always lower than the difference between GRACE and Swarm.
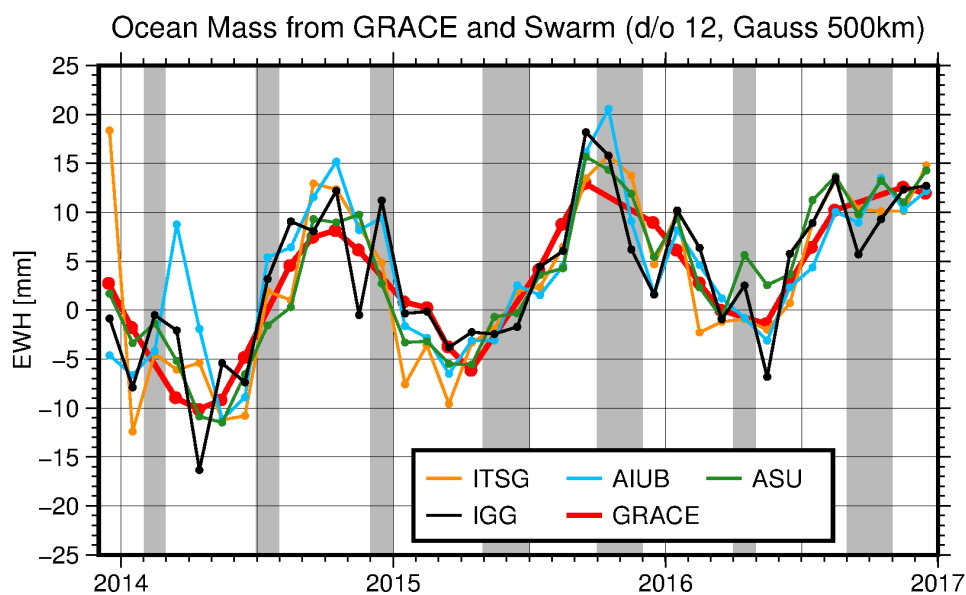
Figure 2. Ocean Mass from ITSG-Grace2016 and Swarm. GRACE data gaps are highlighted in gray.

	AIUB	ASU	IGG	ITSG
Orbit	AIUB	ITSG	ESA	ITSG
Approach	Celestial mechanics approach	Acceleration approach	Short-Arc approach	Short-arc approach
max d/o	70	50	40	60

Table 5. Comparison of Swarm solutions from different institutes: Orbit product, computing method, and maximum degree and order.

	GRACE	AIUB	ASU	IGG	ITSG
GRACE	7.1	5.1	2.8	4.0	5.2
AIUB		8.3	4.5	4.3	5.4
ASU			8.0	4.2	4.1
IGG				8.2	5.6
ITSG					9.0

Table 6. Comparison of RMS [mm] of the individual ocean mass time series (main diagonal) and the RMSE [mm] between two solutions (off-diagonal).

	GRACE	AIUB	ASU	IGG	ITSG
Trend [mm yr^{-1}]	3.5	2.1	4.2	3.3	2.4
Amplitude (annual) [mm]	7.9	7.4	6.9	6.8	9.0
Amplitude (semiannual) [mm]	1.1	2.9	0.5	2.3	1.2
Phase (annual) [days]	-12.0	-12.4	-12.1	-12.8	-12.6
Phase (semiannual) [days]	6.6	13.4	13.7	7.8	-9.9

Table 7. Comparison of Swarm solutions from different institutes: trend, amplitude and phase.
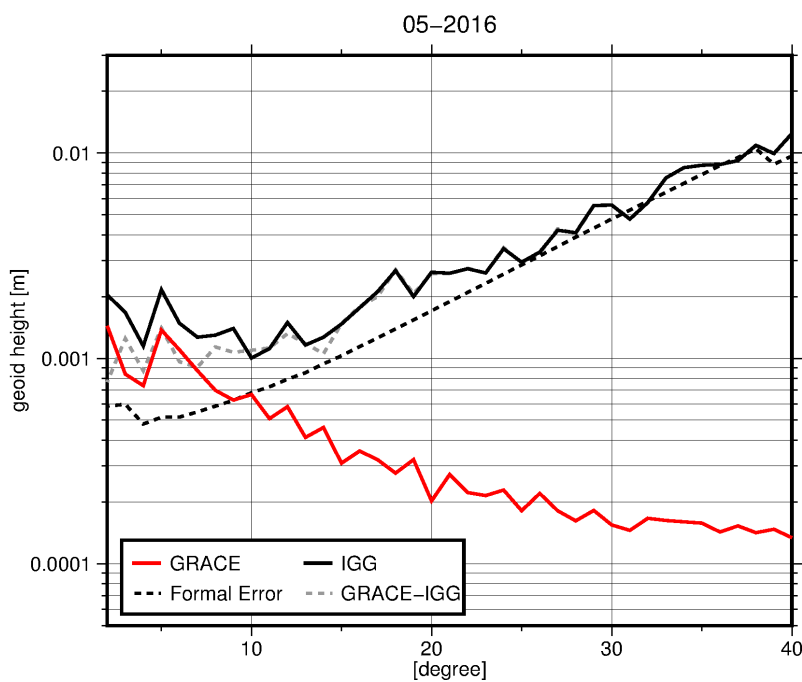
Figure 3. Degree variances for GRACE and Swarm (solution May 2016). Formal errors as well as the difference degree variance (GRACE-Swarm) are shown with dotted lines.
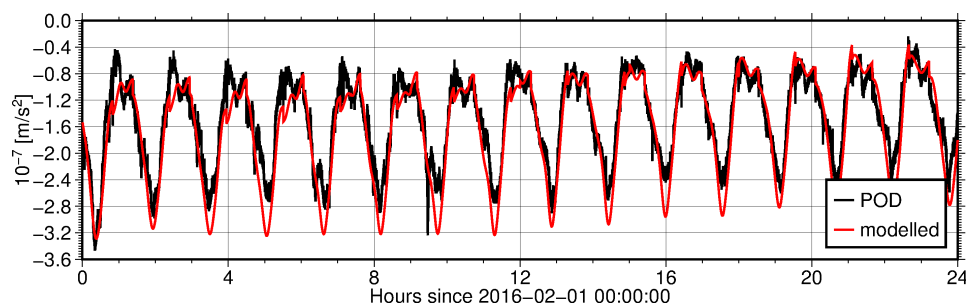
Figure 4. Along-track acceleration of Swarm C
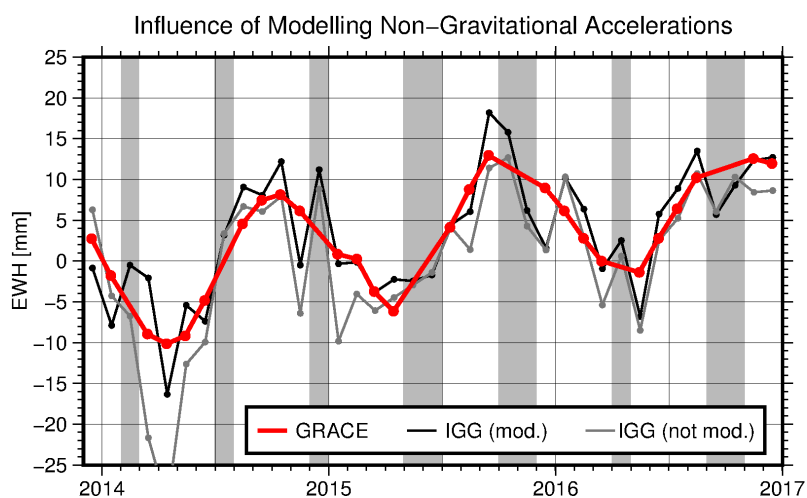
Figure 5. Effect of modelling of non-gravitational forces on ocean mass computation

4.2 Effect of modelling of non-gravitational forces

Figure 4 compares modelled non-gravitational accelerations (see Sect. 3.1) to Siemes et al. (2016) who corrected the accelerometer measurements and improved them with POD. Both time series are very close together, which confirms our intention to use the modelled non-gravitational accelerations for gravity field estimation. Small systematic deviations can be compensated for by co-estimating additional bias or scale parameters.

Modelling non-gravitational accelerations from the Swarm satellites within TVG recovery provides an ocean mass time series significantly closer to the one from GRACE (see Fig. 5) and it also improves the trend estimate as can be seen in Table 8.

	GRACE	IGG	IGG (not mod.)	IGG (trend+annual+semiannual)
Trend [mm/yr]	3.5	3.3	4.0	3.5
Amplitude (annual) [mm]	7.9	6.8	8.3	7.4
Amplitude (semiannual) [mm]	1.1	2.3	2.6	1.9
Phase (annual) [days]	-12.0	-12.8	-13.1	-10.6
Phase (semiannual) [days]	6.6	7.8	3.5	8.7

Table 8. Comparison of different IGG Swarm solutions. IGG: best monthly IGG solution. IGG (not mod.): same parameterization as IGG, but non-gravitational accelerations are not modelled. IGG (trend+annual+semiannual): IGG solution with an estimated trend, annual and semiannual signal per spherical harmonic coefficient.
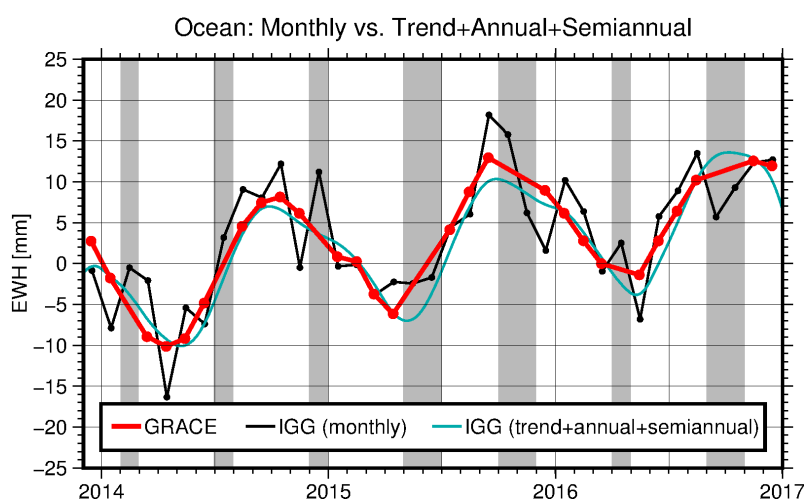
Figure 6. Ocean mass from GRACE and Swarm. The monthly solution is shown in black while the solution with an estimated trend, annual and semiannual signal per coefficient is shown in blue.

4.3 Effect of gravity field parameterization

Figure 6 shows (1) monthly Swarm solutions compared to (2) ocean mass derived with a trend, annual and semiannual signal for each spherical harmonic coefficient. Obviously, the second approach fits much better to the GRACE time series, depicted in red: The RMSE decreases from 4.0 mm for (1) to only 1.7 mm for (2). Furthermore, we find a trend estimate of 3.5 mm yr^{-1}, which is surprisingly close to GRACE (see Table 8). In other words, directly parameterizing trend, annual and semiannual terms for each harmonic coefficient, instead of computing the usual monthly solutions, leads to solutions which are much closer to GRACE. To our knowledge, this has not been investigated for Swarm, prior to this study.
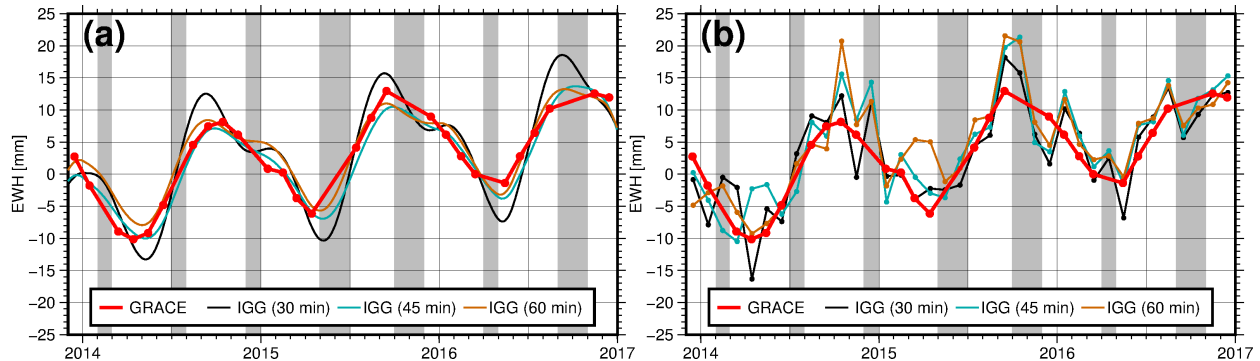
Figure 7. Effect of varying the arc length. (a) Trend+annual+semiannual solution. (b) Monthly solutions.

4.4 Effect of different arc lengths

We investigated the effect of different arc lengths of 30 minutes, 45 minutes and 60 minutes on ocean mass estimates (see Fig. 7). The remaining parameters have been chosen according to our best results. For the approach with trend, annual and semiannual signal terms, the solution with 30 minute arcs differs most from GRACE and the other two solutions, while 45 minute arcs provide the lowest RMSE (1.7 mm) and the best trend estimate (3.5 mm yr^{-1}). When considering monthly solutions, 30 minute arcs provide the best result (RMSE: 4.0 mm and trend: 3.3 mm yr^{-1}).

4.5 Effect of the parameterization of non-gravitational forces

In addition to modelling the non-gravitational forces, which are introduced in the gravity estimation process as accelerometer data, we carried out several tests concerning the co-estimation of "accelerometer bias and scale factors". For both, Fig. 8 (a) and (b), we find that a global scaling factor per axis only has a minor influence. For the solutions with trend, annual and semiannual signal terms, parameterizing the bias as a linear function works better than a constant value per axis. The reason for this might be the large number of observations (10s sampling for 37 months) compared to the low number of parameters. The additional parameters per arc give room for improving not only the modelled non-gravitational accelerations, but also the gravity field parameters. Looking at monthly solutions, we find that a constant bias per axis works better than a linear function. For both, (a) and (b), we also introduced the bias as a constant value or a polynomial of degree 4 for the whole timespan of either 37 months (a) or one month (b). The two solutions do not differ much, but they are of a minor quality compared to other solutions.

4.6 Contribution of Swarm A, B, C

In this study, we combine the information from the three spacecraft by simply accumulating the normal equations. For reasons of interpretation and validation, it makes sense to investigate also the single-satellite solutions. Figure 9 (a) compares ocean mass change derived from the individual monthly solutions to a combination and GRACE, while Fig. 9 (b) shows the solutions estimated with a trend, an annual and a semiannual signal. It is expected that Swarm A and Swarm C provide similar solutions
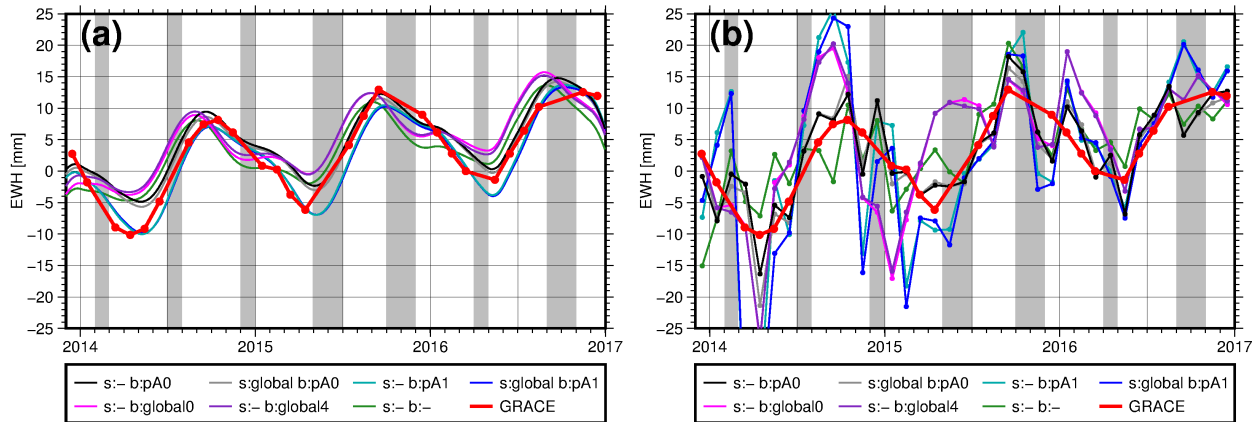
Figure 8. Effect of co-estimating bias and scale factors for the non-gravitational accelerations. Abbreviations: s=scale, b=bias, pA=per arc. The numbers indicate the degree of the polynomial. (a) Trend+annual+semiannual solution. (b) Monthly solutions.
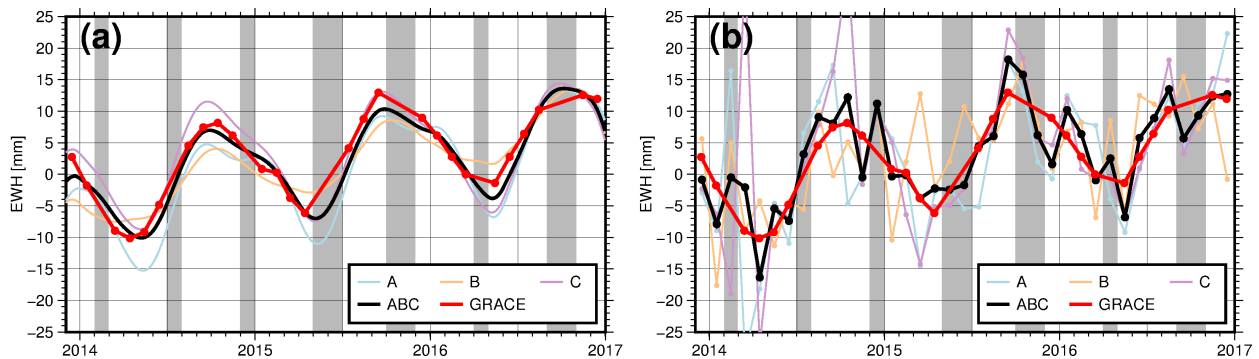
Figure 9. Influence of individual satellites on the combined solution. (a) Trend+annual+semiannual (b) Monthly solutions.

as they fly side by side. This is the case for 9 (a), but it is not always true for the monthly solutions. One possible explanation might be the different receiver settings.

4.7 River basin mass estimates

Even though we concentrated on ocean mass in this study, we also derived river basin mass estimates to validate our TVG
5 results in other regions. We investigated the same parameterizations that we used to derive ocean mass changes (see Table 4).
To assess the solutions with regard to their quality, we compare our results to those derived from the GRACE mission. We
computed the ratio of the root mean square error (RMSE) to the root mean square (RMS) of the GRACE time series. The
RMSE will be calculated with respect to the available GRACE data (27 out of 37 months from December 2013 to December

2016). This will give a kind of inverse signal to noise ratio (1/SNR):

$$\frac{1}{SNR} = \frac{RMSE\left(\overline{F}_{O_W,Swarm}(t)\right)}{RMS\left(\overline{F}_{O_W,GRACE}(t)\right)} \tag{11}$$

Figure 10 shows the 100 best solutions with a direct estimation of trend, annual and semiannual signal terms, while Fig. 11 shows an equal number of the best monthly solutions.

As expected, the ratio of RMSE/RMS is lowest for the ocean, followed by the Amazon basin, which means that these results are the most reliable. Greenland and Ganges mass estimates have RMSE/RMS < 1 for trend+annual+semiannual solutions and they also perform better than Mississippi and Yangtze, when we look at the monthly solutions. It is obvious, that modelling non-gravitational accelerations provides better results than not modelling them. Also, the estimation of a bias seems to be
10 mandatory. In general, the results confirm what has been evaluated in Sect. 4.2 to 4.5.

4.8 Bridging a possible gap with Swarm

As GRACE has met the end of its lifetime, we make efforts here to close the gap until GRACE-FO provides data. We study as well the possibility to fill monthly gaps, which are usually bridged by interpolating the previous and subsequent monthly solutions. To find out, whether Swarm TVG should be preferred to interpolating GRACE data, we assume that existing monthly
15 solutions are missing, such that we are still able to compare to the actual solutions. In Fig. 12 (a) we assumed each GRACE solution to be missing at one time. We then estimated a harmonic time series consisting of mean, trend, annual and semiannual terms from all solutions except for the one that is considered to be missing. This leads to the blue curve. When comparing the interpolated GRACE time series to the Swarm solution, we find that their difference to the real GRACE solution is very close. Nevertheless, it appears still slightly better to close monthly gaps by interpolating than relying on the Swarm solution.

In case of a longer gap between GRACE and GRACE-FO, ocean mass estimates from Swarm will become more important. Figure 12 (b) shows what would happen, if the last six months of GRACE would be missing. The procedure is the same as before, i.e. we estimate a harmonic signal (mean, trend, annual and semiannual) from the remaining GRACE data. This leads to the blue curve, which is further offset from GRACE than our Swarm solution. Over three years, this would also lead to a
25 degradation of the trend estimate (GRACE and Swarm: 3.5 mm yr^{-1} and interpolated GRACE: 4.0 mm yr^{-1}).

We simulated all possible gaps with a duration between 1 month and 18 months in the time series from December 2013 to December 2017 and tested all gap filling methods (interpolating GRACE, using monthly Swarm solutions, using trend+annual+semiannual Swarm solutions). With other words: when we assumed a gap of e.g. 3 months, we investigated gaps from 12-2013 to 02-2014
30 until 10-2016 to 12-2016, which makes 35 possibilities. The mean RMSE with respect to the real GRACE data is shown in Table 9. It is obviously better to use our trend+annual+semiannual solution to fill gaps instead of using monthly solutions. However, for a gap of e.g. three months, we get a mean RMSE of 1.1 mm for interpolating existing GRACE solutions com-
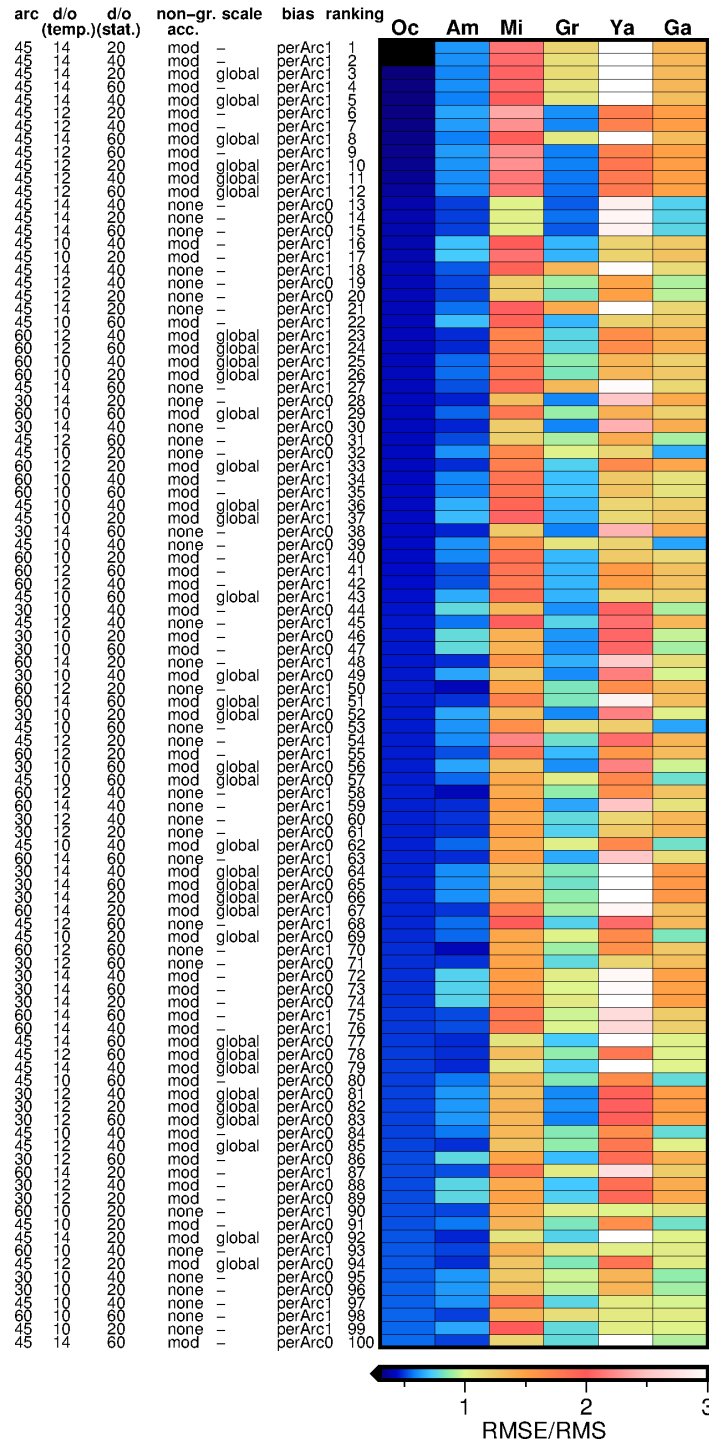
Figure 10. Evaluation of methods (trend+annual+semiannual solutions).
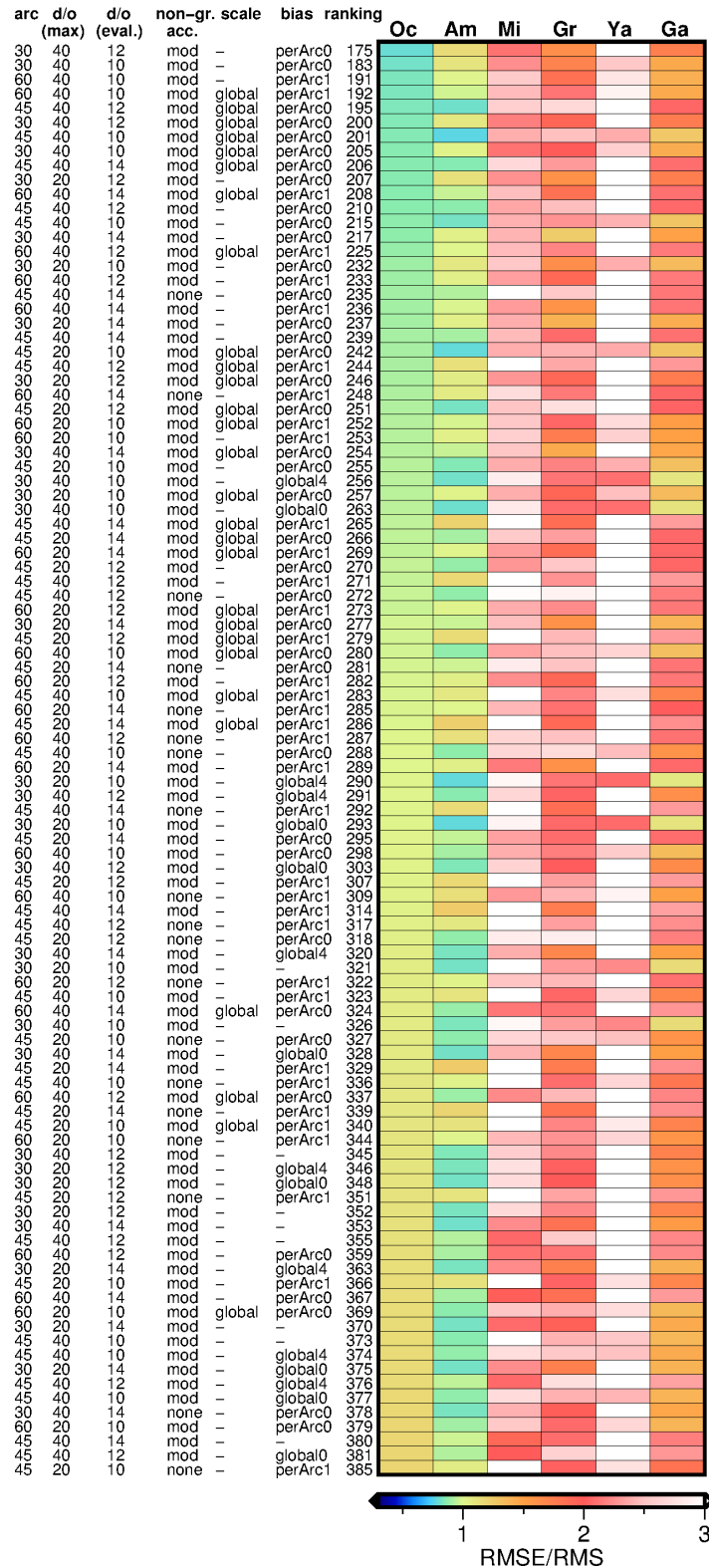
Figure 11. Evaluation of methods (monthly solutions).
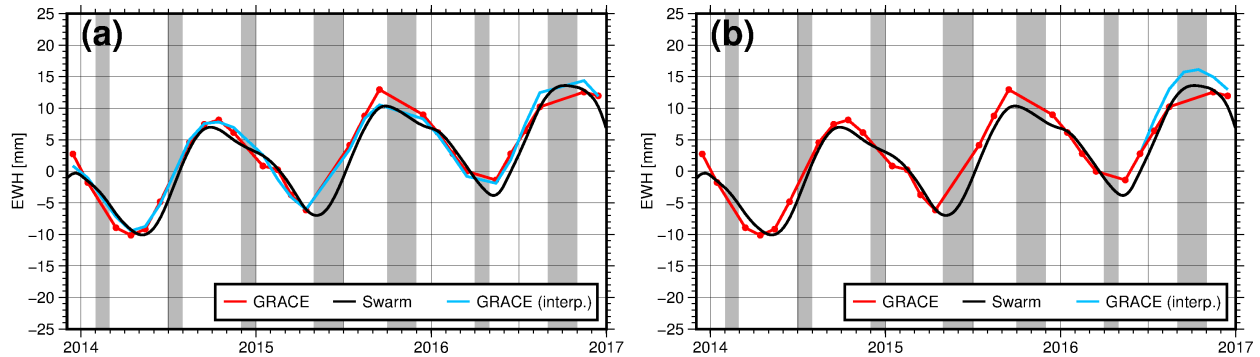
Figure 12. Bridging Gaps with Swarm. Our IGG Swarm solution (black) is compared to the monthly GRACE solutions (red) as well as to interpolated values when we assume a part of the GRACE time series to be missing. (a) Each month is assumed to be missing and is interpolated from all other months. (b) The last six months are assumed to be missing and are interpolated from all other months.

	1	3	6	12	18
GRACE (interpolated)	0.9	1.1	1.1	1.2	1.8
Swarm (trend+annual+semiannual)	1.4 (13.5 %)	1.5 (17.1 %)	1.6 (6.3 %)	1.6 (3.8 %)	1.6 (80.0 %)
Swarm (monthly)	3.3	3.7	3.8	3.9	3.8

Table 9. Mean RMSE [mm] of the gap-filler methods with respect to existing GRACE data. The columns indicate the number of missing months. The percentage of Swarm (trend+annual+semiannual) solutions with a lower RMSE than GRACE (interpolated) solutions is indicated in brackets.

pared to 1.5 mm for the trend+annual+semiannual solution. For a prolonged gap of 18 months, our Swarm solution would, however, be closer to GRACE in 80 % of all cases.

4.9 Is it possible to detect La Niña events with Swarm?

5 Boening et al. (2012) and Fasullo et al. (2013) showed that the 2010/2011 La Niña event led to a 5 mm drop in Global Mean Sea Level (GMSL). This has been derived from satellite altimetry as well as from a combination of GRACE and Argo data. As most of the anomaly has been shown to be caused by mass changes, it is reasonable to ask whether we would have been able to observe the drop in ocean mass with Swarm (or to observe a similar event in the future). A simple computation tells that with an RMSE of 4.0 mm for monthly Swarm solutions, we would be able to detect a 6-months-drop of 4.0 mm $/\sqrt{6} = 1.6$ mm.

10 As the 2010/2011 drop was both larger and lasted longer, we conclude we would have been able, and thus will also be able in the future, to detect La Niña events with Swarm.

We have conducted another simulation experiment with simulated ocean mass data from 1993 to 2004 taken from Wenzel and Schröter (2007) (see Fig. 13). Assuming the Wenzel and Schröter time series as the truth here, we then generate 1000 simulated
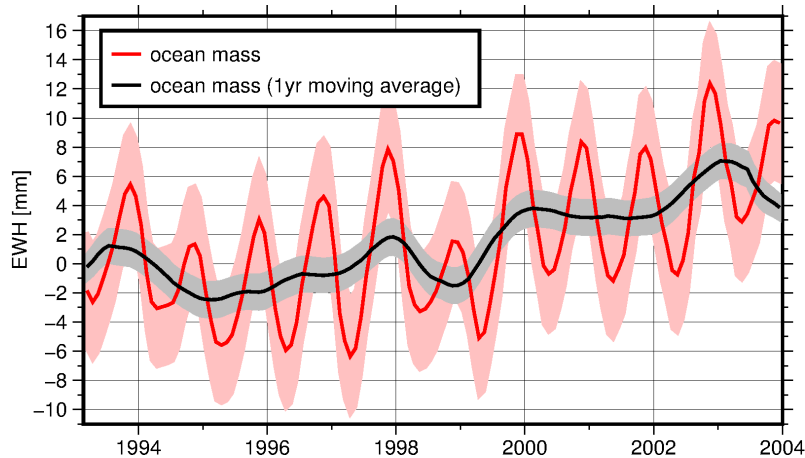
Figure 13. Simulation of the detection of a La Niña event with Swarm. The red curve shows ocean mass from 1993 to 2004. An RMS of 4.0 mm is shaded in pink to simulate Swarm mass estimates. A moving average filter of one year is applied (black) and the resulting standard deviation is shown in gray (simulated ocean mass from Wenzel and Schröter (2007)).

Swarm time series by adding white noise with an RMS of 4.0 mm (pink area). When comparing the filtered (moving average of one year) time series shown as black line with standard deviation of 1.2 mm derived from the simulated Swarm time series (gray), we can clearly identify the drop in the years 1998 to 2000 standing out against the noise floor. Summarized, strong La Niña events such as they occurred in the past could be observed with Swarm, which will be of special importance in case of a prolonged gap between GRACE and GRACE-FO.

5   Conclusions

Swarm-derived ocean mass estimates show the same behavior as those from GRACE, but they appear overall noisier, as expected. IGG monthly solutions have an RMSE with respect to GRACE of 4.0 mm, which is comparable or better than the solutions from other institutions that we investigated (AIUB, ASU, ITSG). Over the Swarm period we find a mass trend of 3.3 mm yr^{-1}, which is close to that from GRACE (3.5 mm yr^{-1}). The spread between the different Swarm solutions is of the same order of magnitude as the RMSE of Swarm with respect to GRACE. As expected prior to launch, the degree variances for monthly solutions suggest that the TVG fields are only reliable up to degree about 12.

In a second approach we estimated a trend, an annual and a semiannual signal term for each spherical harmonic coefficient and for the whole period of time. We find that this significantly improves ocean mass trend estimates; here we obtain an RMSE of 1.7 mm and the same trend as derived from GRACE. We investigated different parameterizations and found that an arc length of 30 minutes provides the best results for monthly solutions, while 45 minutes is the best option for the trend+annual+semiannual solutions. Furthermore, co-estimating an "accelerometer bias" proved to be important. A constant bias per arc and axis works best for monthly solutions and an additional trend parameter is needed for the trend+annual+semiannual approach.

We validated TVG results by computing river basin mass estimates and by again comparing to GRACE. We found that the relation of the RMSE/RMS ratio, which can be considered as a noise-to-signal ratio, is lowest for the ocean, followed by the Amazon basin. Some of the Greenland and Ganges solutions also show a 1/SNR lower than one. Swarm-derived surface mass change over the Yangtze and Mississippi appears worse; the reason is likely (1) that the signal is too weak to be detected from

5   kinematic orbits only, and (2) the basin might be too small.

We showed that La Niña events like those from 2010-2011 and 1998-2000 could have been easily identified with Swarm, which is of special importance for the future after the termination of the GRACE mission. In simulation studies, we tested three different methods for filling the gap that now will occur between GRACE and GRACE-FO, as well as for reconstructing missing single months in the GRACE time series: (1) interpolating existing monthly GRACE solutions, (2) using monthly

10   Swarm solutions, (3) using the trend+annual+semiannual Swarm solution. As expected, (3) provides better results than (2) and whether (1) or (3) is better depends on the length of the gap and on the presence of episodic events and interannual variability. In the (short) Swarm period where ocean mass displayed little variability beyond the annual cycle, we found that for reconstructing either single months or three-month periods (1) may work slightly better than (3), whereas in case of a long 18 month gap, (3) should be preferred.

15   In future work, we will concentrate on improving our ocean mass estimates from Swarm by allowing the trend to change over time as shown e.g. in (Didova et al., 2016). Furthermore, we work towards ingesting our Swarm solutions at the normal equation level into the fingerprint inversion of (Rietbroek et al., 2016), to improve existing sea level budget results and to partition altimetric sea level changes into its different components, even for those periods where we do not have GRACE data.

Data availability.

20   – The GRACE spherical harmonic coefficients that were used for comparison can be found on ftp://ftp.tugraz.at/outgoing/ ITSG/GRACE/ITSG-Grace2016/monthly/.

         – The Swarm spherical harmonic coefficients from ITSG Graz can be found on http://ftp.tugraz.at/outgoing/ITSG/tvgogo/ gravityFieldModels/Swarm/.

         – The Swarm spherical harmonic coefficients from ASU Prague can be found on http://www.asu.cas.cz/~bezdek/vyzkum/

25   geopotencial/index.php

Appendix A

A1

Competing interests. The authors declare that they have no conflict of interest.

Acknowledgements. This study is supported by the Priority Program 1788 "Dynamic Earth" of the German Research Foundation (DFG) - FKZ: KU 1207/21-1. The authors are grateful for the Swarm macro model as well as the calibrated accelerometer data from Christian Siemes (ESA). We furthermore want to thank Christoph Dahle for sending us the Swarm gravity fields from AIUB (Bern).

We appreciate the work of Jose van den IJssel, whose kinematic orbits are available on the ESA FTP server. Thank you to Torsten Mayer-Gürr

5   and his colleagues (ITSG Graz) and Aleš Bezděk (ASU Prague) for providing their gravity solutions online.

References

A, G., Wahr, J., and Zhong, S.: Computations of the viscoelastic response of a 3-D compressible Earth to surface loading: an application to Glacial Isostatic Adjustment in Antarctica and Canada, Geophysical Journal International, 192, 557–572, https://doi.org/10.1093/gji/ggs030, 2013.

5 Bezděk, A., Sebera, J., Teixeira da Encarnação, J., and Klokočník, J.: Time-variable gravity fields derived from GPS tracking of Swarm, Geophysical Journal International, 205, 1665–1669, https://doi.org/10.1093/gji/ggw094, 2016.

Boening, C., Willis, J. K., Landerer, F. W., Nerem, R. S., and Fasullo, J.: The 2011 La Niña: So strong, the oceans fell, Geophysical Research Letters, 39, https://doi.org/10.1029/2012GL053055, l19602, 2012.

Cazenave, A. and Llovel, W.: Contemporary Sea Level Rise, Annual Review of Marine Science, 2, 145–173, https://doi.org/10.1146/annurev-
10   marine-120308-081105, 2010.

Chambers, D. P. and Bonin, J. A.: Evaluation of Release-05 GRACE time-variable gravity coefficients over the ocean, Ocean Science, 8, 859–868, https://doi.org/10.5194/os-8-859-2012, 2012.

Cheng, M., Tapley, B. D., and Ries, J. C.: Deceleration in the Earth's oblateness, Journal of Geophysical Research: Solid Earth, 118, 740–747, https://doi.org/10.1002/jgrb.50058, 2013.

15 Dahle, C., Flechtner, F., Gruber, C., König, D., König, R., Michalak, G., and Neumayer, K.-H.: GFZ GRACE Level-2 Processing Standards Document for Level-2 Product Release 0005, Tech. rep., Deutsches GeoForschungsZentrum, https://doi.org/10.2312/GFZ.b103-12020, 2012.

Didova, O., Gunter, B., Riva, R., Klees, R., and Roese-Koerner, L.: An approach for estimating time-variable rates from geodetic time series, Journal of Geodesy, 90, 1207–1221, https://doi.org/10.1007/s00190-016-0918-5, 2016.

20 Doornbos, E.: Thermospheric Density and Wind Determination from Satellite Dynamics, Dissertation, Delft University of Technology, 2011.

Fasullo, J. T., Boening, C., Landerer, F. W., and Nerem, R. S.: Australia's unique influence on global sea level in 2010–2011, Geophysical Research Letters, 40, 4368–4373, https://doi.org/10.1002/grl.50834, 2013.

Gerlach, C. and Visser, P.: Swarm and gravity: Possibilities and expectations for gravity field recovery, in: Proceedings of the First Swarm International Science Meeting, edited by Danesy, D., Nantes, 2006.

25 Gregory, J. M., White, N. J., Church, J. A., Bierkens, M. F. P., Box, J. E., van den Broeke, M. R., Cogley, J. G., Fettweis, X., Hanna, E., Huybrechts, P., Konikow, L. F., Leclercq, P. W., Marzeion, B., Oerlemans, J., Tamisiea, M. E., Wada, Y., Wake, L. M., and van de Wal, R. S. W.: Twentieth-Century Global-Mean Sea Level Rise: Is the Whole Greater than the Sum of the Parts?, Journal of Climate, 26, 4476–4499, https://doi.org/10.1175/JCLI-D-12-00319.1, 2013.

Jäggi, A., Dahle, C., Arnold, D., Bock, H., Meyer, U., Beutler, G., and van den IJssel, J.: Swarm kinematic orbits and gravity fields from 18
30   months of GPS data, Advances in Space Research, 57, 218 – 233, https://doi.org/http://dx.doi.org/10.1016/j.asr.2015.10.035, 2016.

Knocke, P. C., Ries, J. C., and Tapley, B. D.: Earth radiation pressure effects on satellites, 1988.

Llovel, W., K. Willis, J., Landerer, F., and Fukumori, I.: Deep-ocean contribution to sea level and energy budget not detectable over the past decade, Nature Clim. Change, 4, 1031–1035, https://doi.org/10.1038/nclimate2387, 2014.

Löcher, A.: Möglichkeiten der Nutzung kinematischer Satellitenbahnen zur Bestimmung des Gravitationsfeldes der Erde, Dissertation, Uni-
35   versität Bonn, 2010.

Lombard, A., Garcia-Sanoguera, D., Ramillien, G., Cazenave, A., Biancale, R., Lemoine, J.-M., Flechtner, F., Schmidt, R., and Ishii, M.: Estimation of steric sea level variations from combined GRACE and Jason-1 data, Earth and Planetary Science Letters, 254, 194–202, https://doi.org/10.1016/j.epsl.2006.11.035, 2007.

Mayer-Gürr, T.: Gravitationsfeldbestimmung aus der Analyse kurzer Bahnbögen am Beispiel der Satellitenmissionen CHAMP und GRACE, Dissertation, Universität Bonn, 2006.

Mayer-Gürr, T., Behzadpour, S., Ellmer, K., Kvas, A., Klinger, B., and Zehentner, N.: ITSG-Grace2016 - Monthly and Daily Gravity Field Solutions from GRACE, GFZ Data Services, https://doi.org/http://doi.org/10.5880/icgem.2016.007, 2016.

Montenbruck, O. and Gill, E.: Satellite Orbits: Models, Methods, Applications, Springer, 2005.

Nicholls, R. J. and Cazenave, A.: Sea-Level Rise and Its Impact on Coastal Zones, Science, 328, 1517–1520, https://doi.org/10.1126/science.1185782, 2010.

Olsen, N., Friis-Christensen, E., Floberghagen, R., Alken, P., Beggan, C. D., Chulliat, A., Doornbos, E., da Encarnação, J. T., Hamilton, B., Hulot, G., van den IJssel, J., Kuvshinov, A., Lesur, V., Lühr, H., Macmillan, S., Maus, S., Noja, M., Olsen, P. E. H., Park, J., Plank, G., Püthe, C., Rauberg, J., Ritter, P., Rother, M., Sabaka, T. J., Schachtschneider, R., Sirol, O., Stolle, C., Thébault, E., Thomson, A. W. P., Tøffner-Clausen, L., Velímský, J., Vigneron, P., and Visser, P. N.: The Swarm Satellite Constellation Application and Research Facility (SCARF) and Swarm data products, Earth, Planets and Space, 65, 1, https://doi.org/10.5047/eps.2013.07.001, 2013.

Pail, R., Gruber, T., Fecher, T., and GOCO Project Team: The Combined Gravity Model GOCO05c, GFZ Data Services, https://doi.org/http://doi.org/10.5880/icgem.2016.003, 2016.

Picone, J. M., Hedin, A. E., Drob, D. P., and Aikin, A. C.: NRLMSISE-00 empirical model of the atmosphere: Statistical comparisons and scientific issues, Journal of Geophysical Research: Space Physics, 107, SIA 15–1–SIA 15–16, https://doi.org/10.1029/2002JA009430, 1468, 2002.

Reigber, C.: Zur Bestimmung des Gravitationsfeldes der Erde aus Satellitenbeobachtungen, DGK, Reihe C 137, Verlag der Bayerischen Akademie der Wissenschaften, Mitteilungen aus dem Institut für Astronomische und Physikalische Geodäsie, Nr. 63, 1969.

Rietbroek, R., Fritsche, M., Dahle, C., Brunnabend, S.-E., Behnisch, M., Kusche, J., Flechtner, F., Schröter, J., and Dietrich, R.: "Can GPS-Derived Surface Loading Bridge a GRACE Mission Gap?", "Surveys in Geophysics", 35, 1267–1283, https://doi.org/10.1007/s10712-013-9276-5, 2014.

Rietbroek, R., Brunnabend, S.-E., Kusche, J., Schröter, J., and Dahle, C.: Revisiting the contemporary sea-level budget on global and regional scales, Proceedings of the National Academy of Sciences, 113, 1504–1509, https://doi.org/10.1073/pnas.1519132113, 2016.

Schneider, M.: A general method of orbit determination, Ph.D. thesis, Ministry of Technology, Farnborough, 1968.

Siemes, C., de Teixeira da Encarnação, J., Doornbos, E., van den IJssel, J., Kraus, J., Perešťý, R., Grunwaldt, L., Apelbaum, G., Flury, J., and Holmdahl Olsen, P. E.: Swarm accelerometer data processing from raw accelerations to thermospheric neutral densities, Earth, Planets and Space, 68, 92, https://doi.org/10.1186/s40623-016-0474-5, 2016.

Stocker, T., Qin, D., Plattner, G.-K., Tignor, M., Allen, S., Boschung, J., Nauels, A., Xia, Y., Bex, V., and Midgley, P., eds.: Sea Level Change, book section 13, p. 1137–1216, Cambridge University Press, Cambridge, United Kingdom and New York, NY, USA, https://doi.org/10.1017/CBO9781107415324.026, 2013.

Sutton, E.: Effects of Solar Disturbances on the Thermosphere Densities and Wind from CHAMP and GRACE Satellite Accelerometer Data, Ph.D. thesis, University of Colorado, 2008.

Swenson, S., Chambers, D., and Wahr, J.: Estimating geocenter variations from a combination of GRACE and ocean model output, Journal of Geophysical Research: Solid Earth, 113, https://doi.org/10.1029/2007JB005338, b08410, 2008.

Teixeira da Encarnação, J., Arnold, D., Bezděk, A., Dahle, C., Doornbos, E., van den IJssel, J., Jäggi, A., Mayer-Gürr, T., Sebera, J., Visser, P., and Zehentner, N.: Gravity field models derived from Swarm GPS data, Earth, Planets and Space, 68, 127, https://doi.org/10.1186/s40623-016-0499-9, 2016.

Trenberth, K. E., Fasullo, J. T., and Balmaseda, M. A.: Earth's Energy Imbalance, Journal of Climate, 27, 3129–3144, https://doi.org/10.1175/JCLI-D-13-00294.1, 2014.

van den IJssel, J., Encarnação, J., Doornbos, E., and Visser, P.: Precise science orbits for the Swarm satellite constellation, Advances in Space Research, 56, 1042–1055, https://doi.org/10.1016/j.asr.2015.06.002, 2015.

van den IJssel, J., Forte, B., and Montenbruck, O.: Impact of Swarm GPS receiver updates on POD performance, Earth, Planets and Space, 68, 85, https://doi.org/10.1186/s40623-016-0459-4, 2016.

Vielberg, K., Forootan, E., Lück, C., Löcher, A., and Kusche, J.: GRACE Accelerometer Data Calibration and its Impact on Thermospheric Neutral Density Estimation, subm.

Visser, P.: Space-borne gravimetry: progress, predictions and relevance for Swarm, in: Proceedings of the First Swarm International Science Meeting, edited by Danesy, D., Nantes, 2006.

Wahr, J., Molenaar, M., and Bryan, F.: Time variability of the Earth's gravity field: Hydrological and oceanic effects and their possible detection using GRACE, 103, 30 205–30 230, 1998.

Wang, X., Gerlach, C., and Rummel, R.: Time-variable gravity field from satellite constellation using the energy integral, Geophysical Journal International, 190, 1507–1525, https://doi.org/10.1111/j.1365-246X.2012.05578.x, 2012.

Wenzel, M. and Schröter, J.: The Global Ocean Mass Budget in 1993–2003 Estimated from Sea Level Change, Journal of Physical Oceanography, 37, 203–213, https://doi.org/10.1175/JPO3007.1, 2007.

Zangerl, F., Griesauer, F., Sust, M., Montenbruck, O., Buchert, B., and Garcia, A.: SWARM GPS Precise Orbit Determination Receiver Initial In-Orbit Performance Evaluation, Proceedings of the 27th International Technical Meeting of the Satellite Division of the Institute of Navigation, pp. 1459–1468, 2014.